Experimental Validation of Intelligent MPPT Control for Photovoltaic Energy Chain

Karima Et-Torabi
Laboratory of Energy & Electrical Systems, ENSEM, Hassan II University of Casablanca, Morocco
karima.ettorabi@ensem.ac.ma (corresponding author)

Abdelouahed Mesbahi
Laboratory of Energy & Electrical Systems, ENSEM, Hassan II University of Casablanca, Morocco
a.mesbahi@ensem.ac.ma

Ayoub Nouaiti
Electrical Engineering Department, EST, Moulay Ismail University of Meknes, Morocco
a.nouaiti@umi.ac.ma

Received: 21 December 2024 | Revised: 4 February 2025 | Accepted: 6 February 2025

ABSTRACT

This paper presents a comparative study of two Maximum Power Point Tracking (MPPT) algorithm techniques for a Photovoltaic (PV) system, which includes a PV generator, a DC-DC boost converter, and a resistive load. The study compares the performance of Artificial Neural Networks (ANN) and Perturb and Observe (P&O) algorithms in extracting maximum power under both stable and variable climatic conditions. To this end, simulation tests are performed using MATLAB Simulink, with a focus on energy efficiency and response time in different scenarios. The findings are validated through a hardware setup using the LAUNCHPAD-XL 28F379D and C2000 embedded coder. The results demonstrate that the ANN-based MPPT technique outperforms the traditional P&O method, particularly under rapidly changing environmental conditions, highlighting its superior efficiency in PV systems. Additionally, the ANN algorithm has been shown to exhibit enhanced adaptability to variable irradiance and temperature, thereby ensuring more stable and consistent power output across a broad spectrum of operating conditions.

Keywords-Maximum Power Point Tracking (MPPT); Artificial Neural Networks (ANNs); digital signal processor; Perturb and Observe (P&O); DC-DC converter

I. INTRODUCTION

PV systems are capable of converting sunlight into electricity, thereby providing a sustainable energy source. However, external factors such as solar irradiance and temperature can exert a substantial influence on the performance of these systems. Due to the non-linear behavior exhibited by PV installations, it becomes imperative to implement MPPT methods to extract the maximum possible power under varying environmental conditions. MPPT algorithms are designed to dynamically adjust the operating point of solar panels, thereby optimizing their output and ensuring efficient energy harvesting. A review of the extant literature reveals the existence of numerous MPPT algorithms designed to enhance the performance of PV systems by efficiently extracting power from solar panels. These algorithms include the following: Parasitic Capacitance (PC), Constant Voltage (CV), Incremental Conductance (INC), Hill Climbing (HC), P&O, Fuzzy Logic Control, Particle Swarm Optimization (PSO), and Artificial Neural Network (ANN) control. The efficacy of these methods varies in terms of factors such as stability, convergence speed, cost, implementation complexity, and environmental adaptability [1-14]. Among these, the P&O method is one of the simplest and most widely used MPPT techniques. It perturbs the operating point and observes the resulting power changes. While effective in many scenarios, P&O can experience oscillations, particularly when irradiance changes rapidly [7]. The INC method enhances P&O by dynamically adjusting the operating point based on the power-voltage derivatives, resulting in enhanced tracking performance and reduced susceptibility to rapid irradiance fluctuations [15]. Similarly, the Fractional Open-Circuit Voltage (FOCV) method uses the constant ratio principle of open circuit voltages, demonstrating reduced sensitivity to temperature variations and suitability for diverse environmental conditions [16].

A critical aspect of optimizing PV system performance is ensuring that the DC power output from the solar panels is properly conditioned to be usable for various loads or storage systems. This is where DC-DC converters, particularly the boost converter, play a crucial role. The boost converter raises the low voltage output from the PV array to a higher, more usable level, ensuring that energy can be transferred efficiently to the load or stored in batteries. The boost converter's ability to regulate the output voltage [11, 17], is vital in ensuring consistent energy output, especially in scenarios where the PV array operates at reduced voltages due to suboptimal environmental conditions. This enhances the overall efficiency of the system by compensating for variations in input voltage caused by changes in solar irradiance and temperature. The integration of these converters with MPPT algorithms ensures that the system can dynamically adapt to changing conditions while maintaining a stable, optimal output. The use of artificial intelligence-based algorithms, including ANN and fuzzy logic control, is a promising development. These techniques are capable of adapting to changing conditions without relying heavily on precise system models, making them more flexible and robust in real-world applications. In contrast to conventional methods, AI-based approaches have the capacity to acquire knowledge from environmental data and execute real-time modifications, thereby substantially enhancing system performance in fluctuating conditions [11, 17]. A method for MPPT that uses neural networks and a feedforward multilayer architecture is presented by authors in [18] for use with PV panels mounted on automobile roofs, were shading changes quickly. Using pre-selected data from the PV system, the neural network automatically determines the global MPP. Only the current and voltage (*I* and *V*) variables are used in this procedure. The ANN ability to extract the most energy and increase prediction accuracy improves with the amount of data gathered. Authors in [14] demonstrate that the response of the ANN is significantly influenced by the input variables, which are the output power derivative (*dP*) and voltage derivative (*dV*) corresponding to specific insolation and operating cell temperature conditions. The ANN output variable is the corresponding normalized increasing or decreasing duty cycle (+1 or -1). This paper compares the traditional P&O, MPPT algorithm with an advanced feedforward multilayer ANN-based MPPT algorithm, evaluating their performance under varying conditions. We propose an ANN-based technique that directly predicts the duty cycle (*D*) from photovoltaic power (P_{pv}) measurements. To ensure robustness under irradiation variations, the neural network is trained using a standard P&O response with a small duty cycle step. The custom hardware and software platforms developed for testing are described, and a detailed performance analysis across different solar irradiance levels is provided. The proposed method is experimentally validated using a DSP, demonstrating its effectiveness in real-world applications.

II. THE STUDIED PV SYSTEM

The PV system under study, as presented in Figure 1, comprises a PV panel, a boost converter, a resistive load, and two MPPT algorithms. The PV panel functions as the primary source of electricity, while the boost converter adjusts the voltage to meet the load's demands. The effectiveness of two MPPT algorithms is compared to optimize power extraction under varying environmental conditions.

A. PV Module

The electrical characteristics of the Canadian Solar CS6P-240P PV panel used in this study are enumerated in Table I, measured under Standard Test Conditions (1000 W/m² and 25°C). Figure 2 presents the simulated *I-V* and *P-V* characteristics of the panel.

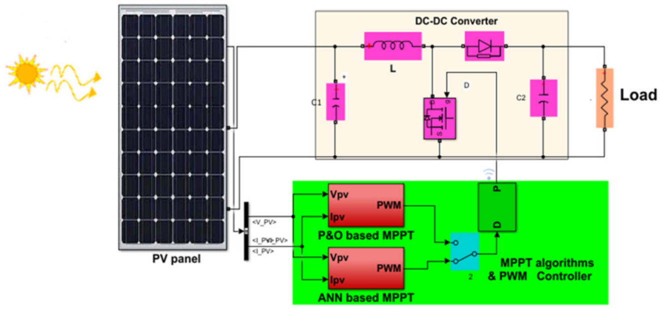

Fig. 1. Block diagram of the studied PV system.

TABLE I. ELECTRICAL CHARACTERISTICS OF THE USED PV

Parameters	Values
Open circuit voltage V_{oc} (V)	37
Short-circuit current I_{sc} (A)	8.59
Current at MPP I_{mp} (A)	8.03
Voltage at MPP V_{mp} (V)	29.9
Maximum Power (W)	240
Temperature coefficient of I_{sc}	0.063
Temperature coefficient of V_{oc}	-0.36
Cells per module (*N*cell)	60

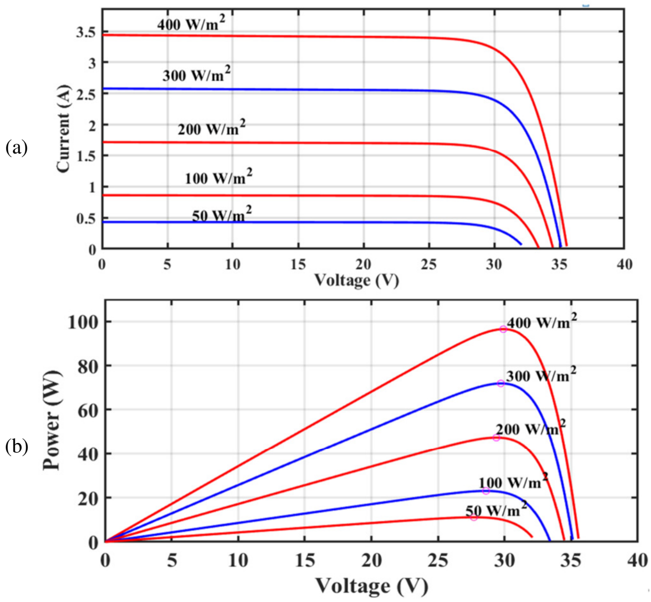

Fig. 2. (a) *I–V* and (b) *P–V* characteristic curve of PV panel under different levels of solar irradiation and constant temperature of 25°C.

B. P&O Method

The P&O algorithm is a simple and widely used MPPT technique. It functions by perturbing the input voltage (V_{pv}) and observing the resulting changes in the power output (P_{pv}) from the PV generator. Despite its simplicity, the P&O method can suffer from oscillations, especially under rapidly changing irradiance conditions. The conventional P&O implementation is shown in Figure 3 [1, 19-21].

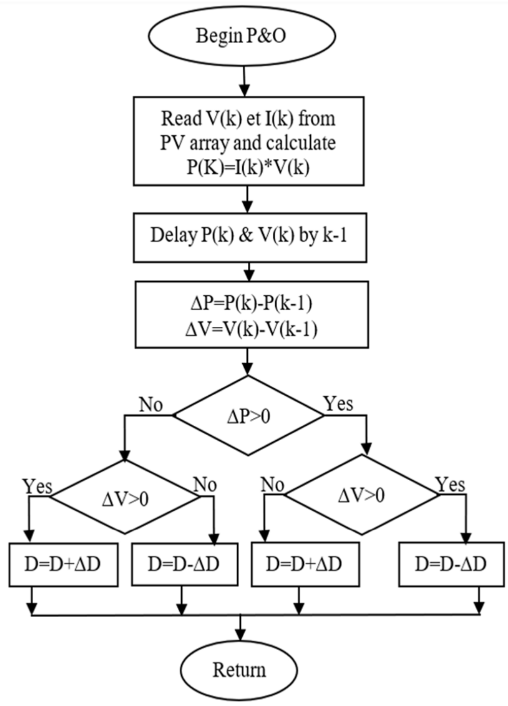

Fig. 3. Flowchart of P&O algorithm.

C. MPPT based ANN

ANNs are designed to emulate the functionality of biological neurons and necessitate training through the usage of input/target pairs. Among the various feedforward neural network architectures, the Multilayer Perceptron (MLP) [4, 22] has gained significant popularity. In the present study, a three-layer neural network configuration was employed, comprising an input layer with a single neuron, a hidden layer comprising 10 neurons, and an output layer [17].

The input parameter is indicated by P_{pv}, and the output parameter is defined as D.

$$n_i^1 = \sum_{i=1}^{10} w_i \times X + b_i^1 \tag{1}$$

where w_i is the weight between the input $X = [P_{pv}]$ and the hidden layer neurons, b^{ih} is the bias for the hidden layer neurons, with i = 1, 2...10, as presented in Figure 4. The following is derived from hidden layer neurons [4, 22]:

$$a_i^1 = f_1(\sum_{i=1}^{10} w_i \times X + b_i^1) \tag{2}$$

$$f_1(n) = tansig(n) = \frac{2}{1+e^{-2n}} - 1 \tag{3}$$

These models can be used to calculate the output of the ANN:

$$n_k^2 = \sum_{j=1}^{10} w_j \times a_j^1 + b_k^2 \tag{4}$$

$$y_k = f_2\left(\sum_{j=1}^{10} w_j \times a_j^1 + b_k^2\right) \tag{5}$$

$$f_2(n) = purelin(n) = n \tag{6}$$

where w_j represents the weight between the output and the hidden layer, and b^2_k is the bias weight.

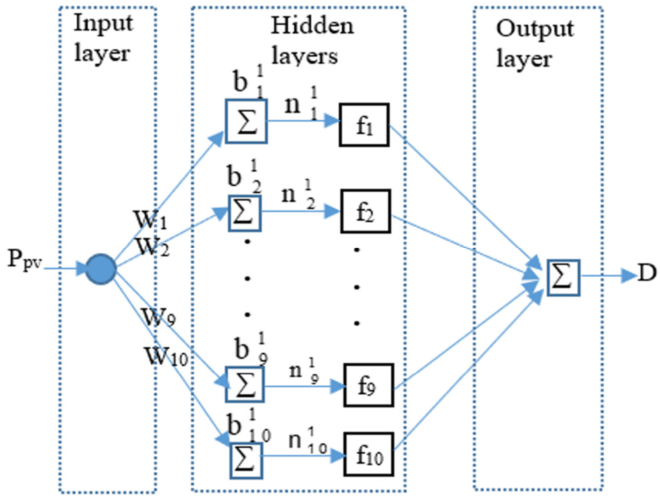

Fig. 4. The proposed neural network architecture.

The samples were generated in a MATLAB simulation using the corrected P&O algorithm. While the full simulation yields 500,001 samples, 90 samples were selected for the final analysis. The dataset consists of three parts: 15% for validation, 70% for training, and 15% for testing. The MSE plot of the ANN model's performance is shown in Figure 5. The regression plot demonstrates a strong correlation during the training, testing, and validation phases of the ANN model. Additionally, the network's outputs and the desired outcomes are perfectly linked when the regression (R) values are close to 1. Levenberg-Marquardt is one of the fastest and most accurate algorithms for solving nonlinear least squares problems [22]. The formula for calculating the MSE is:

$$MSE = \frac{1}{n}\sum_{i=1}^{n}\left(y_i^{actual} - y_i^{predict}\right)^2 \tag{7}$$

where n is the number of input data, y_i^{actual} is the real output, and $y_i^{predict}$ is the target output.

III. SIMULATION RESULTS

To assess the efficacy of the MPPT controls under investigation, a series of numerical simulations were conducted. The system was modeled and simulated using MATLAB/Simulink, as presented in Figure 6. The DC-DC boost converter functions in continuous conduction mode with a switching frequency of 24 kHz. The inductor is modeled as L = 10 mH, the input capacitance as C_1 = 390 µF, the output capacitance as C_2 = 470 µF, and the resistive load as R = 40Ω.

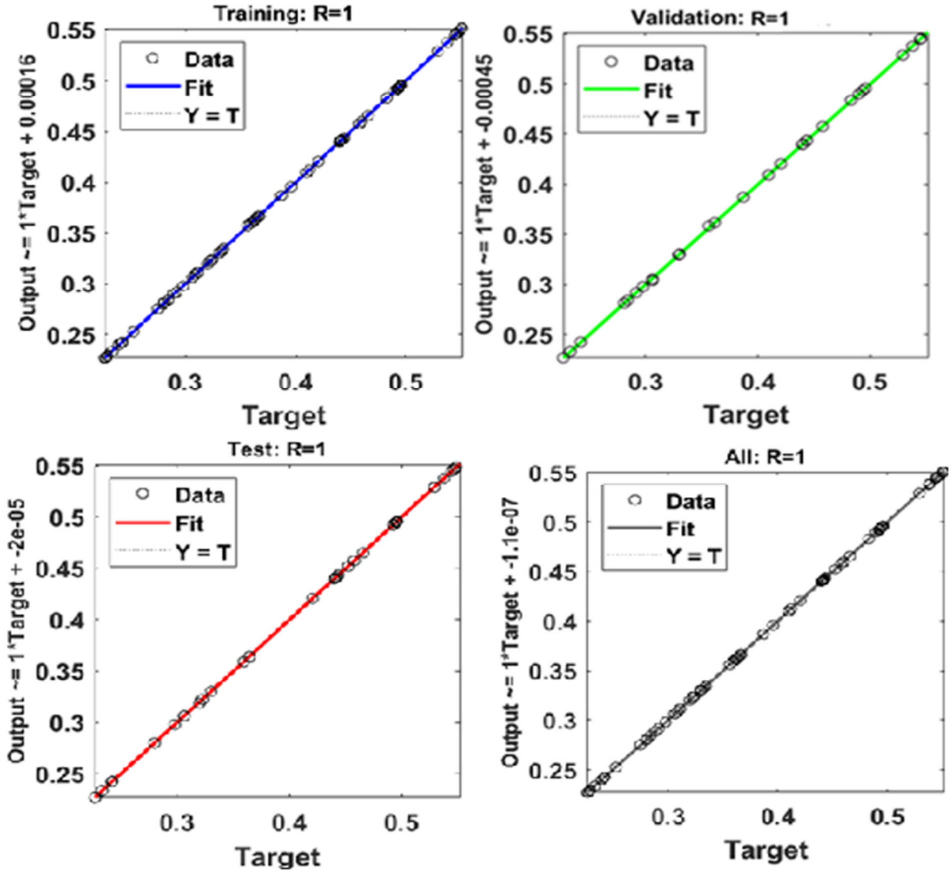

Fig. 5. ANN model performance.

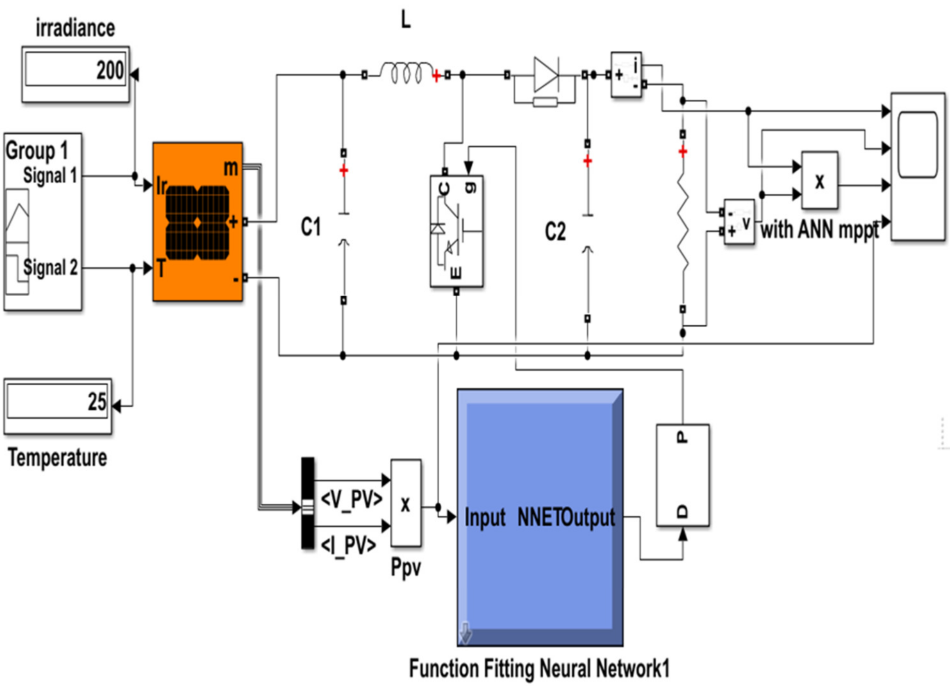

Fig. 6. Simulation model of the studied system.

The irradiance profile is represented in Figure 7. Figure 8 shows the results of the generated PV powers by the ANN and the P&O algorithms, depending on the solar irradiance. In the initial case, the PV system generates a maximum power of 91.6 W at a temperature of 25 °C and a solar radiation intensity of 400 W/m^2, which corresponds to the predicted optimum power. Subsequently, at 25 °C and 100 W/m^2, the PV system attains its predicted optimum power of 17.6 W. Finally, at 25 °C and 50 W/m^2, the PV system generates a maximum power of 3.4 W, aligning with the predicted optimum power. The simulation outcomes thus demonstrate that, in the event of sudden fluctuations in solar radiation conditions, the PV system exhibits a remarkable precision in converging to its optimum power.

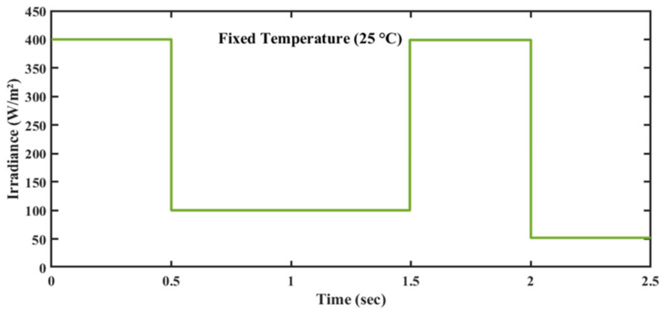

Fig. 7. Irradiance varies between four different levels.

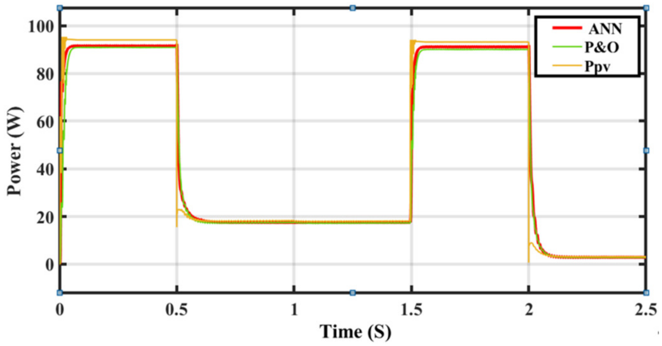

Fig. 8. The generated PV powers by the ANN and the P&O.

In Figure 9, the proximate views are used to illustrate the improvements in output power, response time, and tracking speed achieved using both algorithms. As indicated by Figure 9, P&O controllers demonstrate a response time of 0.038 s to variations in irradiation, while ANN-MPPT controllers exhibit a response time of 0.02 s. The efficiency of each controller is evaluated through the usage of (12) [1, 15]:

$$\eta_{MPPT} = \frac{\int_0^t P_{actual}(t)dt}{\int_0^{t\int} P(t)_{max}} \tag{12}$$

The results demonstrate that the steady-state response of the system does not exhibit oscillations. Moreover, the ANN algorithm produces significantly lower power ripples compared to the conventional P&O algorithm. The implementation of the ANN algorithm has been shown to enhance the MPPT tracking efficiency from 98.50% to 99.50%. Additionally, the ANN algorithm has been demonstrated to exhibit excellent tracking rapidity, particularly around the MPP, ensuring enhanced performance under dynamic conditions.

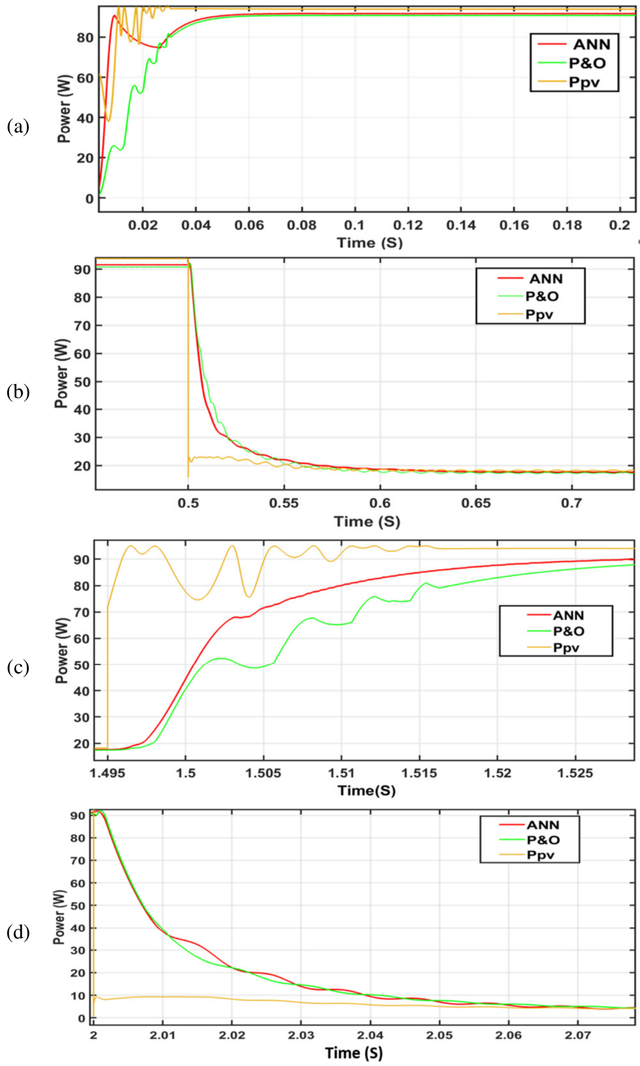

Fig. 9. An approximate comparison of output power using P&O and ANN methods for MPPT :(a) 0 s to 0.2s, (b) 0.4 s to 0.75 s, (c) 1.4 s to 1.53s, (d) 2 s to 2.08 s.

IV. EXPERIMENTAL RESULTS

The hardware configuration of the proposed work is shown in Figure 10. It consists of a 240 Wc PV panel, a boost converter, and a resistive load. The P&O and ANN algorithms were implemented on LAUNCHPAD-XL 28F379D. Figure 11 presents the Simulink implementation using C2000 blocks. The Simulink model was constructed, and the generated code was loaded onto the microcontroller through Code Composer Studio. The currents (I_{pv}, I_{out}) and voltages (V_{pv}, V_{out}) required for this work were sensed using LA 55-P and LV 25-P, respectively. To acquire digital values of I_{pv}, I_{out}, V_{pv}, and V_{out}, ADCx is employed. The ePWM block generates pulses according to the duty cycle calculated by the MPPT algorithm. The switching frequency was fixed at 25 kHz.

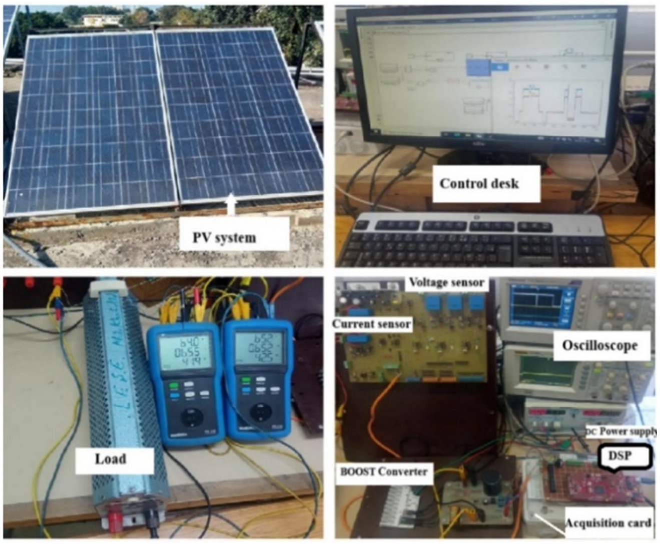

Fig. 10. The experimental hardware used in our lab.

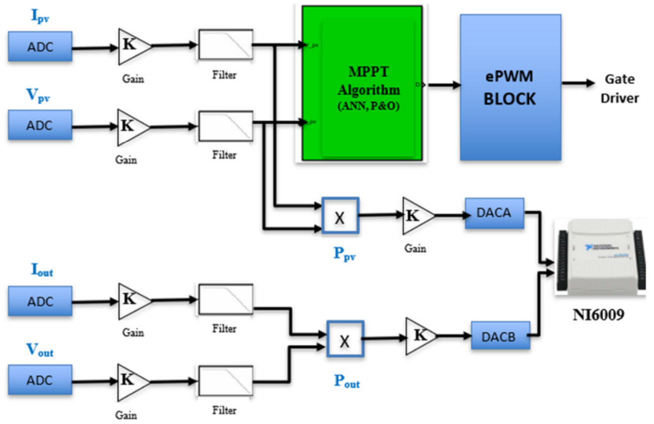

Fig. 11. Program for acquiring data using the DSP F28379D and processing the data with MATLAB-Simulink.

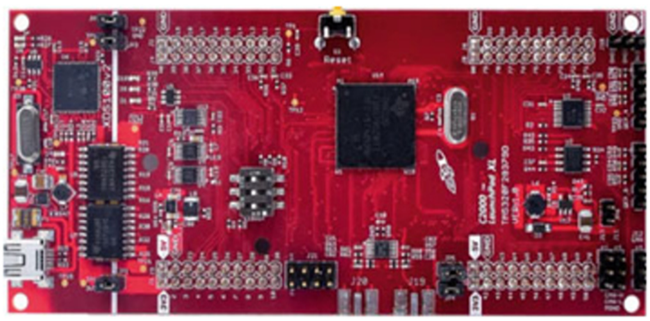

Fig. 12. TMS320F28379D Launchpad.

As shown in Figure 12, the control card is equipped with a dual-core 32-bit microcontroller that possesses DSP capabilities. Key components include General-Purpose Input/Output (GPIO) pins, an Analog-to-Digital Converter (ADC), a Digital-to-Analog Converter (DAC), and an ePWM module. Collectively, these components facilitate precise control and efficient signal processing for a wide range of applications [23]. In order to ascertain the effectiveness of the MPPT controllers under conditions of partial shading, the PV panel is covered with a board which was subsequently removed. During the experiment, the PV panel was subjected to varying levels of shading, as shown in Figure 13, in order to analyze its performance under different conditions.

Initially, between 14 and 50 s, the PV panel remains fully uncovered, operating at its maximum potential. From 50 to 60 s, 50% of the panel was covered, reducing its exposure to light. Between 60 and 75 s, 90% of the panel was covered. This staged shading setup allows for observing the tracking performance of PV systems under partially shaded conditions. Using the ANN algorithm, the system can swiftly and efficiently track the MPP, even in the presence of changing shading levels and variable loads. We conducted the same experiment using the P&O algorithm, with the results presented in Figure 14.

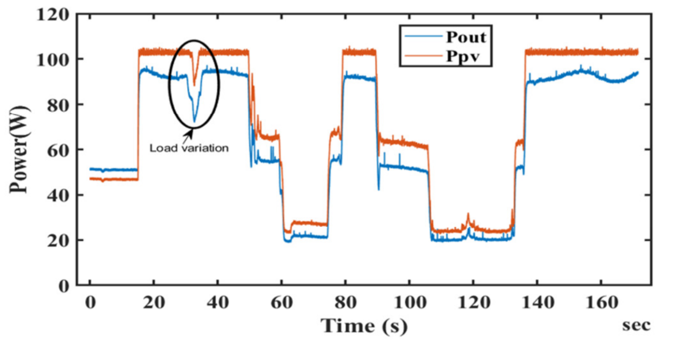

Fig. 13. Experimental power for ANN control under different irradiances.

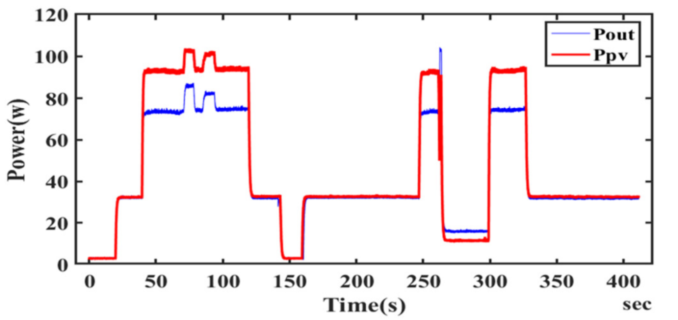

Fig. 14. Experimental power for P&O control under different irradiances.

During the initial interval, ranging from 49 s to 130 s, the PV panel wasis fully exposed to light, thereby enabling it to function at its maximum capacity. In this interval, the output load undergoes a change at 90 s and 100 s, introducing dynamic variations. In the subsequent period, from 130 s to 140 s, a segment of the panel becomes shaded, leading to a reduction in its light exposure and consequent alteration in its output. Between 140 and 160 s, 90% of the panel was shaded. This experimental configuration underscores the efficacy of the P&O algorithm in tracking the MPP under conditions of variable load and shading. The waveforms under consideration of Figures 13 and 14 were compared, and as shown in Figure 15, it is evident that the output power reaches the maximum power of the PV system. According to Figure 15, the PV power produced using the P&O controller and the ANN controller is 85.51 W and 90 W, respectively. The ANN controller has been proved to reduce steady-state oscillations and enable faster tracking. The experimental results demonstrate that the MPPT tracking efficiency with the ANN algorithm is 96.5%, which is significantly higher than the 87.91% efficiency achieved with the P&O algorithm. However, it should be noted that the MPPT tracking efficiency may be susceptible to tracking errors and loss of direction during sudden changes in solar irradiation.

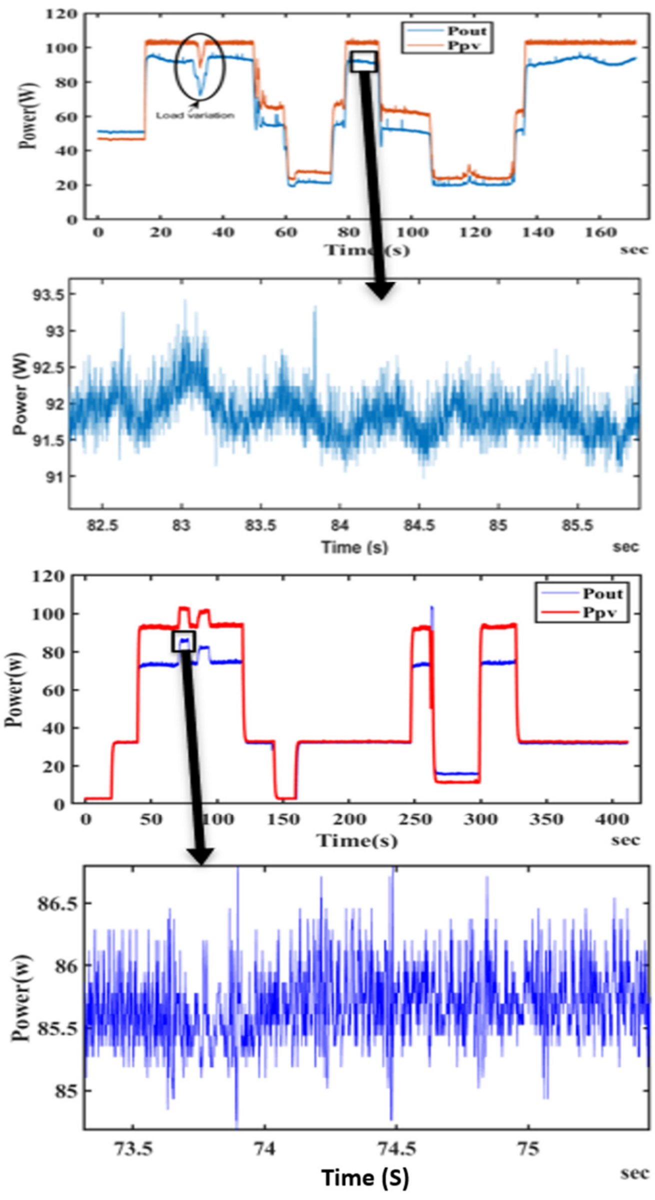

Fig. 15. An approximate comparison of experimental power using P&O and ANN methods for MPPT.

Table II presents a summary of the calculated efficiency, network architecture, input variables, and operating conditions from the literature on MPPT using ANN techniques. The table presents the efficiency levels attained in each study, with the highest efficiency recorded at 99.5%. The observed variability in efficiency values and the conditions under which they were attained underscores the impact of diverse input variables and the system's adaptability to changing environmental conditions. These disparities offer significant insights into the efficacy and optimization of ANN-based MPPT methods.

TABLE II. SUMMARIES OF KEY STUDIES FROM THE LITERATURE ON MPPT USING ANN TECHNIQUES

Ref	Network architecture	Input variables	Conditions	Efficiency
This paper	Multilayer feedforward	P_{pv}	Variable irradiation	99,5%
[14]	Multilayer feedforward	dP and dV	variable	-
[18]	Backpropagation momentum	V and I	variable	98,47%
[24]	Feedforward	T and G	variable	97%
[25]	Single layer	T and G	uniform	-

V. CONCLUSIONS

This study compared two Maximum Power Point Tracking (MPPT) tracking strategies for Photovoltaic (PV) panels: the Perturb and Observe (P&O) and Artificial Neural Networks (ANN) algorithms, both implemented on a Digital Signal Processor (DSP). The results demonstrated that while the P&O algorithm is effective under stable irradiance, it struggles with rapid changes. In contrast, the ANN algorithm provides faster and more accurate tracking in dynamic conditions. Although the P&O algorithm works well in uniform conditions, its performance declines under partial shading. The integration of the ANN algorithm could enhance MPPT efficiency across a wider range of conditions. Future research could explore further optimization of the ANN algorithm for diverse environmental factors, potentially improving PV system performance in real-world applications.

REFERENCES

[1] A. O. Baba, G. Liu, and X. Chen, "Classification and Evaluation Review of Maximum Power Point Tracking Methods," *Sustainable Futures*, vol. 2, Jan. 2020, Art. no. 100020, https://doi.org/10.1016/j.sftr.2020.100020.

[2] D. Mazumdar, C. Sain, P. K. Biswas, P. Sanjeevikumar, and B. Khan, "Overview of Solar Photovoltaic MPPT Methods: A State of the Art on Conventional and Artificial Intelligence Control Techniques," *International Transactions on Electrical Energy Systems*, vol. 2024, no. 1, 2024, Art. no. 8363342, https://doi.org/10.1155/2024/8363342.

[3] M. L. Katche, A. B. Makokha, S. O. Zachary, and M. S. Adaramola, "A Comprehensive Review of Maximum Power Point Tracking (MPPT) Techniques Used in Solar PV Systems," *Energies*, vol. 16, no. 5, Jan. 2023, Art. no 2206, https://doi.org/10.3390/en16052206.

[4] S. Motahhir, A. El Hammoumi, and A. El Ghzizal, "The most used MPPT algorithms: Review and the suitable low-cost embedded board for each algorithm," *Journal of Cleaner Production*, vol. 246, Feb. 2020, Art. no. 118983, https://doi.org/10.1016/j.jclepro.2019.118983.

[5] M. Bouksaim, M. Mekhfioui, and M. N. Srifi, "Design and Implementation of Modified INC, Conventional INC, and Fuzzy Logic Controllers Applied to a PV System under Variable Weather Conditions," *Designs*, vol. 5, no. 4, Dec. 2021, Art. no. 71, https://doi.org/10.3390/designs5040071.

[6] V. Jately, B. Azzopardi, J. Joshi, B. Venkateswaran V, A. Sharma, and S. Arora, "Experimental Analysis of hill-climbing MPPT algorithms under low irradiance levels," *Renewable and Sustainable Energy*

Reviews, vol. 150, Oct. 2021, Art. no. 111467, https://doi.org/10.1016/j.rser.2021.111467.

[7] S. Ahmed, S. Mekhilef, M. Mubin, K. S. Tey, and M. Kermadi, "An Adaptive Perturb and Observe Algorithm With Enhanced Skipping Feature for Fast Global Maximum Power Point Tracking Under Partial Shading Conditions," *IEEE Transactions on Power Electronics*, vol. 38, no. 9, pp. 11601–11613, Sep. 2023, https://doi.org/10.1109/TPEL.2023.3285243.

[8] A. Saberi, M. Niroomand, and B. M. Dehkordi, "An Improved P&O Based MPPT for PV Systems with Reduced Steady-State Oscillation," *International Journal of Energy Research*, vol. 2023, no. 1, 2023, Art. no. 4694583, https://doi.org/10.1155/2023/4694583.

[9] F. Yahiaoui *et al.*, "An Experimental Testing of Optimized Fuzzy Logic-Based MPPT for a Standalone PV System Using Genetic Algorithms," *Mathematical Problems in Engineering*, vol. 2023, no. 1, 2023, Art. no. 4176997, https://doi.org/10.1155/2023/4176997.

[10] M. N. Ali, K. Mahmoud, M. Lehtonen, and M. M. F. Darwish, "An Efficient Fuzzy-Logic Based Variable-Step Incremental Conductance MPPT Method for Grid-Connected PV Systems," *IEEE Access*, vol. 9, pp. 26420–26430, 2021, https://doi.org/10.1109/ACCESS.2021.3058052.

[11] H. Ahessab, A. Gaga, and B. Elhadadi, "Enhanced MPPT controller for partially shaded PV systems using a modified PSO algorithm and intelligent artificial neural network, with DSP F28379D implementation," *Science Progress*, vol. 107, no. 4, Oct. 2024, Art. no. 00368504241290377, https://doi.org/10.1177/00368504241290377.

[12] V. H. Nguyen, H. Nguyen, M. T. Cao, and K. H. Le, "Performance Comparison between PSO and GA in Improving Dynamic Voltage Stability in ANFIS Controllers for STATCOM," *Engineering, Technology & Applied Science Research*, vol. 9, no. 6, pp. 4863–4869, Dec. 2019, https://doi.org/10.48084/etasr.3032.

[13] O. Boubaker, "MPPT techniques for photovoltaic systems: a systematic review in current trends and recent advances in artificial intelligence," *Discover Energy*, vol. 3, no. 1, Dec. 2023, Art. no. 9, https://doi.org/10.1007/s43937-023-00024-2.

[14] S. Messalti, A. Harrag, and A. Loukriz, "A new variable step size neural networks MPPT controller: Review, simulation and hardware implementation," *Renewable and Sustainable Energy Reviews*, vol. 68, pp. 221–233, Feb. 2017, https://doi.org/10.1016/j.rser.2016.09.131.

[15] A. Harrison, E. M. Nfah, J. de Dieu Nguimfack Ndongmo, and N. H. Alombah, "An Enhanced P&O MPPT Algorithm for PV Systems with Fast Dynamic and Steady-State Response under Real Irradiance and Temperature Conditions," *International Journal of Photoenergy*, vol. 2022, no. 1, 2022, Art. no. 6009632, https://doi.org/10.1155/2022/6009632.

[16] F. Z. Kebbab, L. Sabah, and H. Nouri, "A Comparative Analysis of MPPT Techniques for Grid Connected PVs," *Engineering, Technology & Applied Science Research*, vol. 12, no. 2, pp. 8228–8235, Apr. 2022, https://doi.org/10.48084/etasr.4704.

[17] K. Et-torabi and A. Mesbahi, "MPPT Based Artificial Neural Network Versus Pertub & Observe For Photovoltaic Energy Conversion System," *E3S Web of Conferences*, vol. 336, 2022, Art. no. 00044, https://doi.org/10.1051/e3sconf/202233600044.

[18] S. A. Rizzo and G. Scelba, "ANN based MPPT method for rapidly variable shading conditions," *Applied Energy*, vol. 145, pp. 124–132, May 2015, https://doi.org/10.1016/j.apenergy.2015.01.077.

[19] M. Kamran, M. Mudassar, M. R. Fazal, M. U. Asghar, M. Bilal, and R. Asghar, "Implementation of improved Perturb & Observe MPPT technique with confined search space for standalone photovoltaic system," *Journal of King Saud University - Engineering Sciences*, vol. 32, no. 7, pp. 432–441, Nov. 2020, https://doi.org/10.1016/j.jksues.2018.04.006.

[20] C. B. N. Fapi, H. Tchakounté, M. A. Hamida, P. Wira, and M. Kamta, "Enhanced P&O MPPT Algorithm based on Fuzzy Logic for PV System: Brief Review and Experimental Implementation," *International Journal of Engineering Science and Application*, vol. 7, no. 4, pp. 105–116, Dec. 2023.

[21] G. Yüksek and A. N. Mete, "A P&O Based Variable Step Size MPPT Algorithm for Photovoltaic Applications," *Gazi University Journal of Science*, vol. 36, no. 2, pp. 608–622, Jun. 2023, https://doi.org/10.35378/gujs.1050325.

[22] M.-F. Tsai, C.-S. Tseng, K.-T. Hung, and S.-H. Lin, "A Novel DSP-Based MPPT Control Design for Photovoltaic Systems Using Neural Network Compensator," *Energies*, vol. 14, no. 11, Jan. 2021, Art. no. 3260, https://doi.org/10.3390/en14113260.

[23] C. Boutahiri, A. Nouaiti, A. Bouazi, and A. M. Hsaini, "Experimental Test of a Three-Phase Inverter Using a Launchpad TMS320F28379D Card," in *Proceedings of the 3rd International Conference on Electronic Engineering and Renewable Energy Systems*, Saidia, Morocco, 2023, pp. 451–459, https://doi.org/10.1007/978-981-19-6223-3_49.

[24] S. Ahmed, H. M. Muhammad Adil, I. Ahmad, M. K. Azeem, Z. e Huma, and S. Abbas Khan, "Supertwisting Sliding Mode Algorithm Based Nonlinear MPPT Control for a Solar PV System with Artificial Neural Networks Based Reference Generation," *Energies*, vol. 13, no. 14, Jan. 2020, Art. no. 3695, https://doi.org/10.3390/en13143695.

[25] Z. Zecevic and M. Rolevski, "Neural Network Approach to MPPT Control and Irradiance Estimation," *Applied Sciences*, vol. 10, no. 15, Jan. 2020, Art. no. 5051, https://doi.org/10.3390/app10155051.